POAC'13
Espoo, Finland

Proceedings of the 22nd International Conference on
Port and Ocean Engineering under Arctic Conditions
June 9-13, 2013
Espoo, Finland

COMPARISON OF MEASURED AND SIMULATED SHORT TERM ICE LOADS ON SHIP HULL

Mikko Suominen [1], Biao Su [2], Pentti Kujala [1], Torgeir Moan [2]

[1]Aalto University, Espoo, FINLAND

[2] Norwegian University of Science and Technology, Trondheim, NORWAY

ABSTRACT

Ship operations in ice are increasing as the interest in transport and oil and gas production in the Arctic is increasing. In order to ensure the safety at sea, the structure of ships has to be designed to withstand the ice induced loads on the ship hull. Therefore knowledge on local ice loads on ships is required. The knowledge on local ice loads has been gained through several full scale measurements in the past in which the frames of ships have been instrumented with strain gauges for local ice loads measurements. These measurements are the basis for current structural design methods. Full scale measurements are the only way to gain reliable data on ice loads on ships. However full scale measurements are lacking because they are expensive to obtain and ship specific. Furthermore, full scale measurements are obtained after building of the ship and therefore serve only for future design. Developing a reliable numerical method would enable to estimate the local ice loads in the design phase and improve the structural design of the ship. In order to establish a numerical method for the design, the method has to be validated with the full scale measurements on different ships.

In this paper, a recently developed numerical method is compared with the full scale measurements conducted on board the Polar Research and Supply Vessel S.A. Agulhas II in the Baltic Sea during March 2012. Short term local ice loads on a frame are simulated with the numerical method by using the ship parameters, operational parameters and the measured ice conditions during the full scale measurements as an input. The simulated local ice loads at the bow are then compared with the measured local ice loads on the bow frame.

INTRODUCTION

The oil and gas production and maritime transportation are increasing in the Arctic. Ice conditions in the Arctic waters increase the requirements for the ship hull. The hull has to withstand the ice induced loads without risking the safety at seas. Therefore the knowledge on ice induced loads on the ship hull is required in the design phase to secure the design of a safe structure.

The ice loads on ship hulls has been measured in full scale in the past as the full scale measurements are the only reliable way to gain knowledge on ice induced loads. The lack in full scale measurements is that measurements are ship specific and the loads can be measured and determined only after the ship has been build. Therefore the knowledge gained from the measurements can be used only for the design of the future ships with the similar main dimensions and operational profile. Developing a reliable numerical method would enable the designers to estimate the ice loads the ship under design would encounter during the operation

in different types of ice conditions. In order to be a reliable numerical method, the method has to be validated with different ships having different main dimensions and different operational profiles.

A numerical method has been recently developed to investigate the global and local ice loads and the performance of a ship in level ice (Su, 2011). The method has been used to simulate global ice loads and ship's performance in ice. The simulations were compared with the full scale measurements on board IB Tor Viking II and the comparison showed a good agreement (Su et al., 2010). Furthermore the local loads on frames were calculated and compared with the full scale measurements on board MT Uikku and the loads were shown to be comparable (Su et al. 2011a). The method has also been used to evaluate the statistics of ice induced frame loads (Su et al., 2011b). The results of the study were plausible, as the simulated ice loading histories on a frame were comparable with the full-scale measurements as well as the statistical distributions for the load amplitudes.

On March 2012 a new full scale ice trial was conducted on board Polar Supply and Research Vessel (PSRV) S.A. Agulhas II. During the measurements, the time histories of ice loads on the ship hull and propulsion system, noise and vibration in different areas of the ship and ship's motions were recorded, and human comfort was studied on the bridge. In addition, underwater noise resulting from the ice breaking was measured. The ice conditions were observed visually and ice thickness was measured with an electromagnetic device and a new stereo camera system. The mechanical properties of ice such as the flexural and compressive strength were also measured.

In this paper, the measured local ice loads on a frame at the bow, will be compared with the ice loads determined with the numerical method. The comparison will be conducted statistically through comparing the number of ice loads, maximum ice loads, mean value, standard deviation and through plotting positions. The Weibull plotting positions are used as suggested by Makkonen (2008).

DESCRIPTION AND INSTRUMENTATION OF THE SHIP

The full scale measurements were conducted on board PSRV S.A. Agulhas II during the ice trial of the ship on March 2012. The ship was built at Rauma Shipyard and was delivered in April 2012. The main dimensions of the ship are presented in Table 1. The ship was built to Polar ice class PC 5 and hull strength according to DNV ICE-10.

Table 1. The main dimensions of the ship.

Length, bpp.	121.8	m
Breath, mould.	21.7	m
Draught, design	7.65	m
Deadweight at design displacement	5000	t
Speed, service	14.0	kn

Before the ice trial, in total nine frames were instrumented to measure the ice induced loading on the ship hull; two at the bow, three at the bow shoulder, and four at the aft shoulder, see Figure 1. In addition, the ice induced stress on the hull plating was measured with two strain sensors at the bow, two sensors at the bow shoulder, and six sensors at the aft shoulder. The instrumentation of the frames and hull plating is presented in Figure 1. The data was recorded with 200 Hz during the whole ice trial and saved into 5-minute time histories. All together 24

hours of operations in ice were conducted and the measurement system was running the whole time.

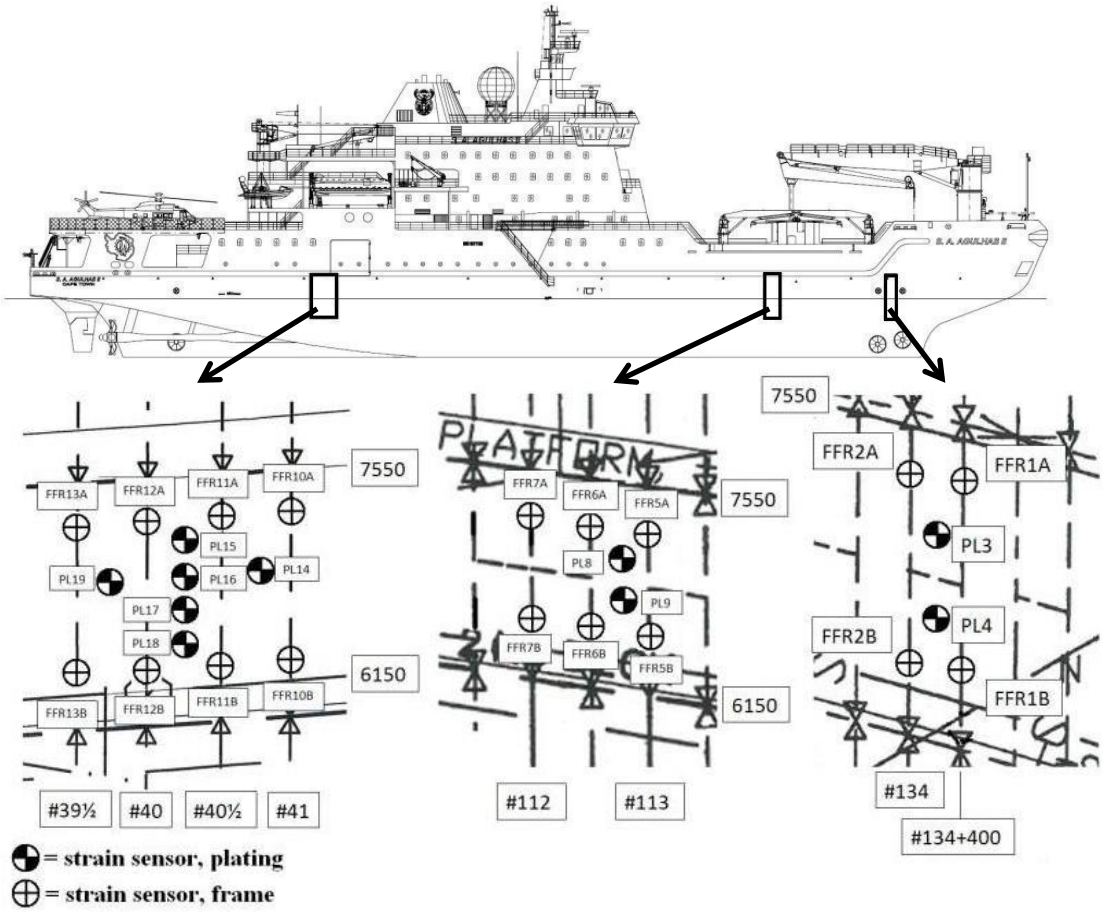

Figure 1. Instrumented hull areas and instrumentation in the areas.

DESCRIPTION OF THE METHOD

As introduced in Su (2011), a numerical method for predicting global and local ice loads on ships has been developed at CeSOS, NTNU. This model is partly based on the empirical data, and a 2D simulation program has been established to reproduce the observed icebreaking patterns and the continuous ice loading processes in a uniform level ice sheet and the ice with randomly varying thickness and strength properties. The basic geometric model for this simulation includes the waterline of the ship and the edge of the ice, both of them are discretized in a 2D plane. Herein each hull node is defined by the x-y location and a hull surface angle, φ; each ice node is defined by the x-y location and ice thickness, h_i. The local ice-hull contact forces are numerically detected and the global ice load is obtained as the integrated value of local ice loads over the hull area. The three degree-of-freedom (3DOF) rigid body equations of surge, sway and yaw are solved by numerical integration, and iterations are performed at each time step to find a balance between the indentation into ice and the resulting ice loads.

The hydrodynamic effects (drag and added mass) on the ship's motion are derived from a numerical calculation before the simulation in ice. The icebreaking forces (crushing and bending) are numerically simulated and the resistance induced by the broken ice pieces (rotating and sliding) is derived from the Lindqvist's formulation (Lindqvist, 1989). The

detailed descriptions of the applied methodology, tools and parameters can be found in Su et al. (2010).

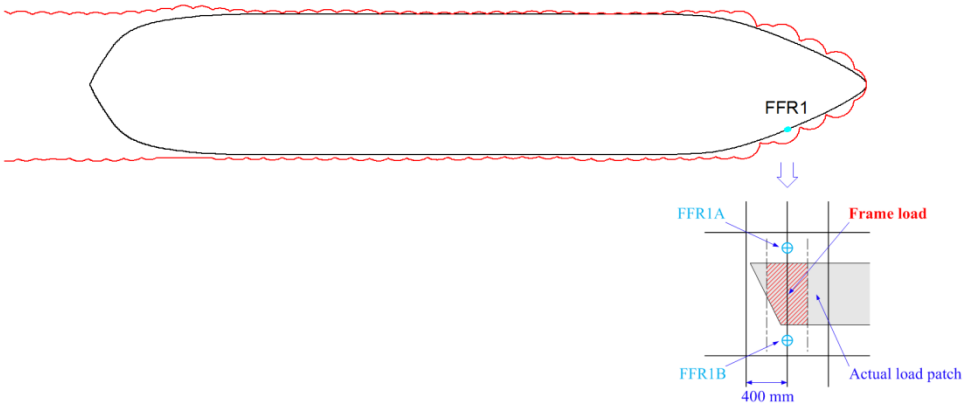

Figure 2. An illustration of the ice-induced frame loads.

In this paper, the numerical model introduced above is applied to investigate the ice-induced loads at the bow (FFR1, as shown in Figure 1 and Figure 2) of S.A. Agulhas II. The short-term ice loads are simulated by using the visually observed ice conditions during full-scale ice trials, and the recorded time series of ship speed are used to determine the course of the ship instead of solving the equations of ship's motion. Figure 3 shows an example of the recorded time histories of ship speed from a full-scale ice trial, the ship's course during this trial and the simulated icebreaking pattern are shown in Figure 4.

Figure 5 shows an example of the simulated time histories of ice loads in a uniform ice condition. By considering the variation of measured ice thickness and strength properties, the simulated ice loading processes (as shown in Figure 6, Figure 7 and Figure 8) would be more representative as compared with field measurements (as shown in Figure 9). In this simulation, the thickness and strength properties of the ice are assumed to be normally distributed along the course of the ship by using the measured and observed mean and standard deviation values given in Table 2 and Table 3. As the standard deviation of ice thickness was not measured during each test, the assumed values (0.1, 0.2 and 0.3×mean ice thickness) are used in each simulation.

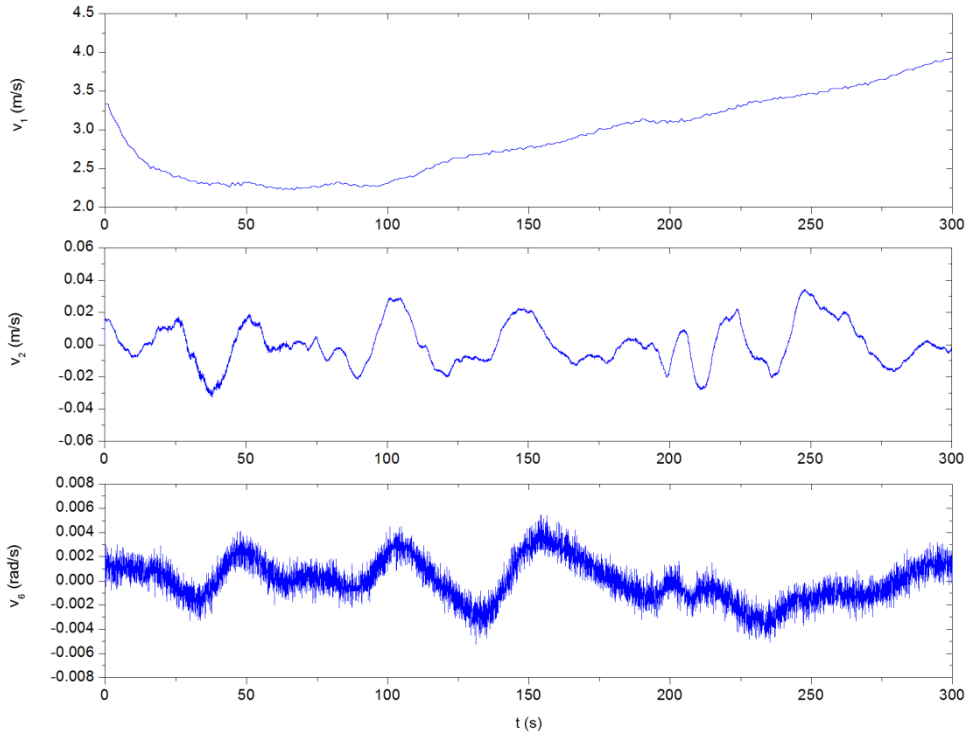

Figure 3. An example of the recorded time histories of ship speed (v1: surge; v2: sway; v6: yaw) from a full-scale ice trial (2012-03-21-06:30).

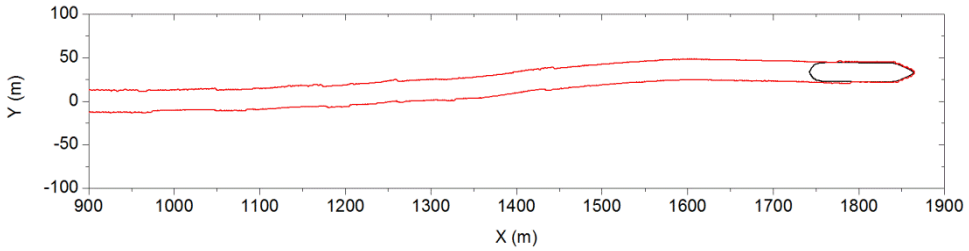

Figure 4. Ship's course and simulated icebreaking pattern (2012-03-21-06:30).

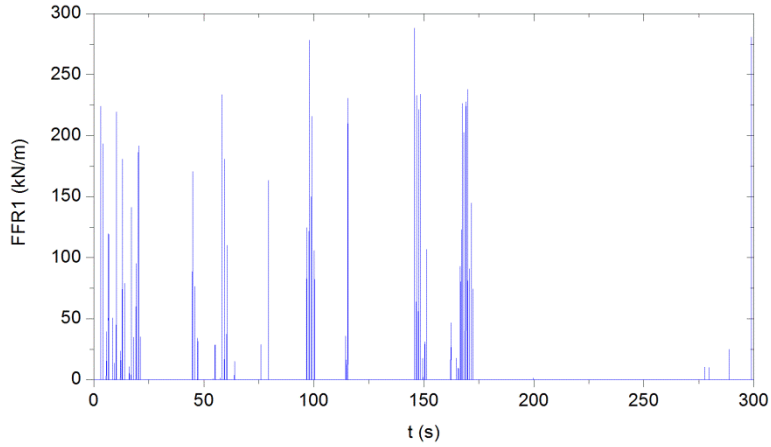

Figure 5. An example of the simulated time histories of ice loads on frame #134+400 (FFR1) in a uniform ice condition (average ice thickness: 0.468 m).

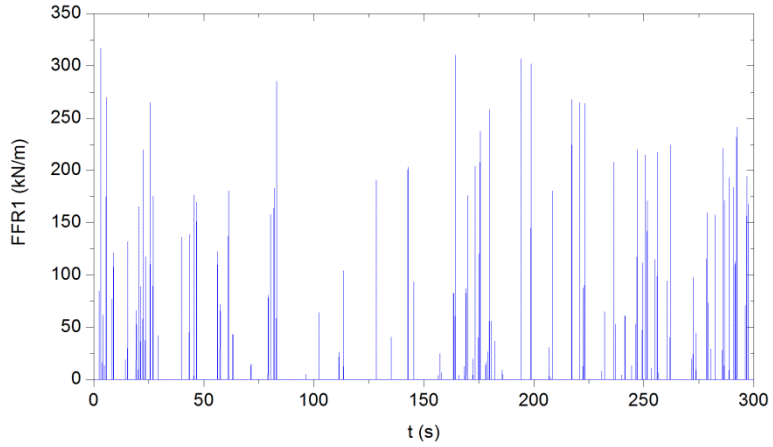

Figure 6. An example of the simulated time histories of ice loads on frame #134+400 (FFR1) in random ice conditions (average ice thickness: 0.468 m; standard deviation: 0.1×0.468 m).

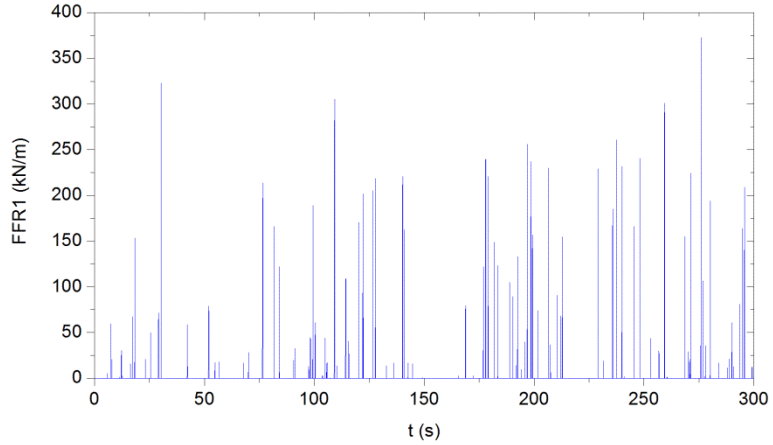

Figure 7. An example of the simulated time histories of ice loads on frame #134+400 (FFR1) in random ice conditions (average ice thickness: 0.468 m; standard deviation: 0.2×0.468 m).

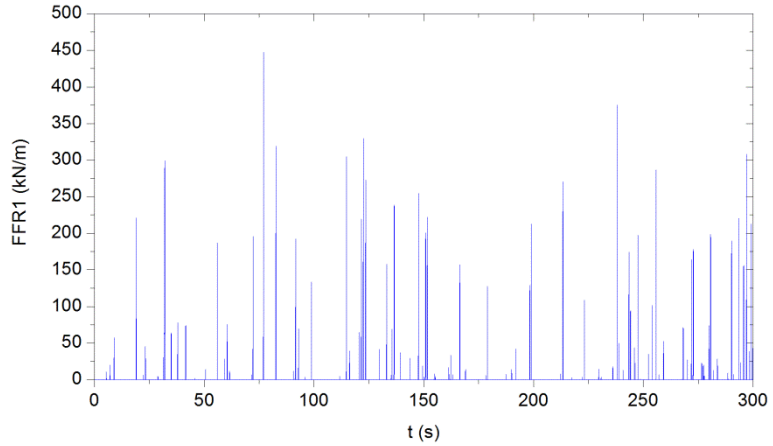

Figure 8. An example of the simulated time histories of ice loads on frame #134+400 (FFR1) in random ice conditions (average ice thickness: 0.468 m; standard deviation: 0.3×0.468 m).

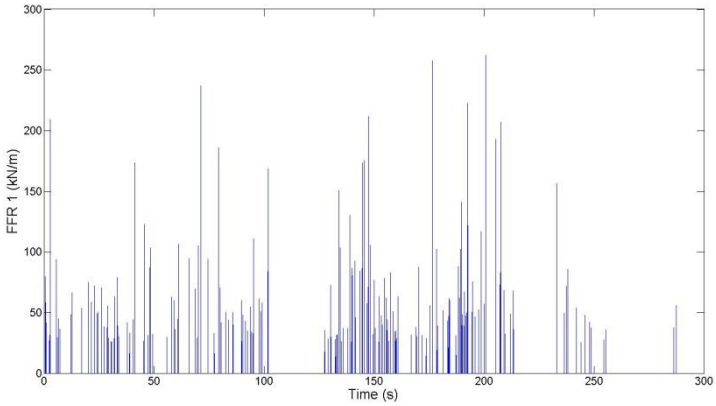

Figure 9. An example of the recorded time histories of ice loads on frame #134+400 (FFR1) from a full-scale ice trial (2012-03-21-06:30) (average ice thickness: 0.468 m).

Table 2. Measured ice strength properties.

	Mean value	Standard deviation
Flexural strength	404 kPa	59 kPa
Horizontal compressive strength	1.28 MPa	0.38 MPa
Vertical compressive strength	2.02 MPa	0.52 MPa

Table 3. Mean ice thickness (selected).

Time stamp	Average ice thickness
2012-03-21-06.15	0.230 m
2012-03-21-11.55	0.287 m
2012-03-21-12.00	0.348 m
2012-03-21-10.15	0.410 m
2012-03-21-06.30	0.468 m

COMPARISON OF THE MEASURED AND SIMULATED LOADS

In this chapter the 5-minute measured and numerically calculated short term ice loads are compared. In total five cases were simulated and compared with the measured ice loads. At first in this chapter, the processing of the measured and calculated ice load time histories and the comparison method are presented. At the end of the chapter the comparison is conducted.

Processing and comparison methods

At first, ice load histograms are produced from the 5-minute measured and calculated time histories. The ice load peaks are identified from the time histories through using Rayleigh separation. Rayleigh separation is based on the comparison of minimum and maximum values. At first, the first maximum value is selected from the load time history. The next maximum value cannot be found until the load values have decreased under the value of the Rayleigh separator. In the measurements on board PSRV S.A. Agulhas II, the separator value was set to be ½, which means, that a value beneath half of the first maximum value must be reached before the second maximum can be selected. If the values of the time history do not decrease under this limit, but instead increase afterwards to greater values than the first value, the first value is abandoned and a new value is chosen to be the first maximum value. Furthermore, only positive maximum values were accepted.

In case of noise, the signal fluctuates around zero when actual ice loads do not occur. As the method compares maxima with minima, a plenty of small loads close to zero are selected. In order to neglect the selected load peaks resulting from noise a threshold for line loads was set to 10 kN/m. This means that load peaks below 10 kN/m are not accepted as ice load peaks.

After the ice loads are identified from time histories, the ice loads are gathered in 5-minute histograms, see Figure 12. In addition, the mean value and the standard deviation are determined for each 5-minute time period separately.

In order to compare the measured and calculated data statistically, the data is presented statistically with the Weibull formula for plotting positions as proposed to be used by Makkonen (2008)

$$p_e = \frac{m}{N+1} \qquad (1)$$

Where *m* is the number of ice loads in a load class and *N* is the total number of the ice loads in the sample. In cumulative distribution, *m* is the cumulative number of the ice loads in load classes.

The sensitivity of simulation

In the simulations, the ice thickness was modelled uniformly (constant ice thickness) and normally distributed by using visually estimated ice thickness as the mean value, μ, and three different standard deviation values which were determined by multiplying the mean value with the ratios of 0.1, 0.2 and 0.3. The sensitivity of simulated ice loads for the standard deviation of ice thickness is studied by comparing these four simulations in between. In the comparison, the mean value of ice thickness is the same in all four simulations. Figure 10 presents the sensitivity of statistically presented ice loads for the used standard deviations.. Figure 10 is produced using Equation (1) for the two simulated 5-minute ice load histograms (Case 6.15 and Case 6.30, see Table 3). As can be seen from this figure, the difference of the cumulative probability between the simulated ice loads by using different standard deviations is greatest for the line loads below 100 kN/m. The difference of the cumulative distribution is insignificant, especially for greater loads, as the curves for the same mean values follow each other closely.

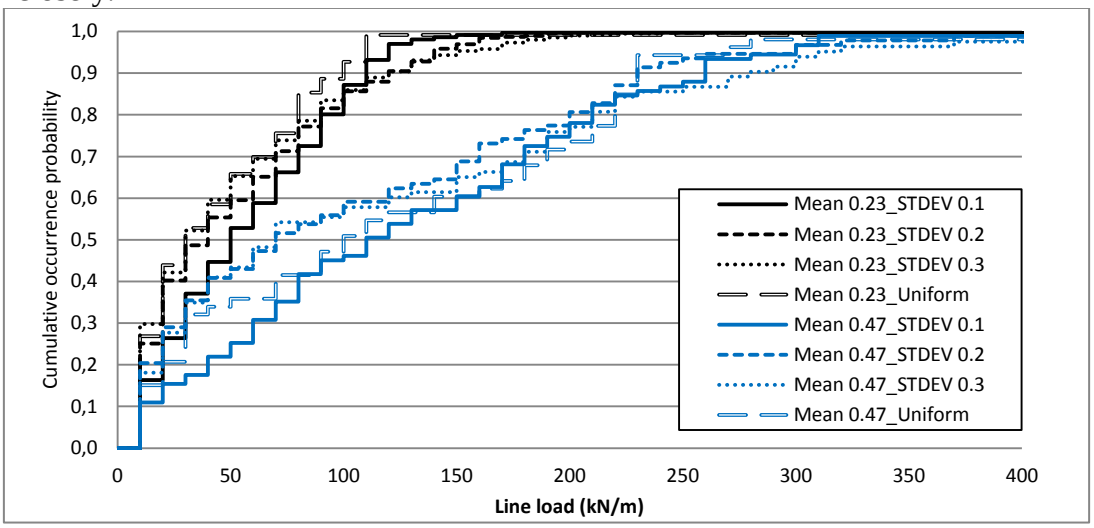

Figure 10. Sensitivity of ice load statistics for the modelled ice conditions. In the label, Mean 0.23 and 0.47 refers to the mean ice thickness and STDEV 0.1, 0.2 and 0.3 refers to the used multiplier in the determination of standard deviation. The ice conditions presented with the standard deviation are modelled normally distributed and the labels Uniform represent constant ice conditions.

Table 4 presents the number of ice load peaks, the maximum ice loads, the mean value and standard deviation of the same cases as presented in Figure 10. As can be seen from Table 4,

the number of ice load peaks clearly increases when the ice conditions are modelled normally distributed. In addition, the simulated maximum ice load and standard deviation of ice loads increase as a function of the standard deviation of ice thickness. As the mean value of ice thickness was visually estimated, the ice thickness variations were not recorded during the whole ice trail and the simulated ice loads by using the normally distributed ice properties do not differ significantly when presented statistically, a median standard deviation value (0.2 times the mean value) of ice thickness was chosen to be used for the following comparison.

Table 4. The effect of ice parameters on the statistical parameters of simulated ice loads. The mean ice thickness in Case 6.15 was 0.23 meters and 0.47 meters in Case 6.30.

		Uniform	STDEV 0.1	STDEV 0.2	STDEV 0.3
Case 6.15	Number of peaks	122	366	389	405
	Max (kN/m)	118.82	170.67	205.42	247.58
	Mean (kN/m)	48.35	61.63	57.56	55.21
	Standard deviation (kN/m)	33.41	37.40	44.40	47.67
Case 6.30	Number of peaks	52	90	92	82
	Max (kN/m)	288.28	316.68	372.97	447.23
	Mean (kN/m)	119.39	130.07	107.44	117.63
	Standard deviation (kN/m)	87.45	87.28	91.50	106.22

Comparison

Figure 11 presents the statistical comparison of the measured and simulated ice loads for all five cases, see Table 3. The mechanical properties in the simulations were modelled normally distributed with the parameters presented in Table 2. The number in the label refers to the time stamp (Case number). The cases are ordered based on increasing mean ice thickness, Case 6.15 being the thinnest (0.23m) and Case 6.30 being the thickest (0.47m), see Table 3. The comparison of the measured and simulated ice loads by using plotting positions shows that the cumulative probability of the simulated ice loads are closer to the measured ice loads in smaller ice thicknesses as the difference of the measured and simulated probability curves for the corresponding cases are closer to each other in smaller ice thicknesses, see Figure 11.

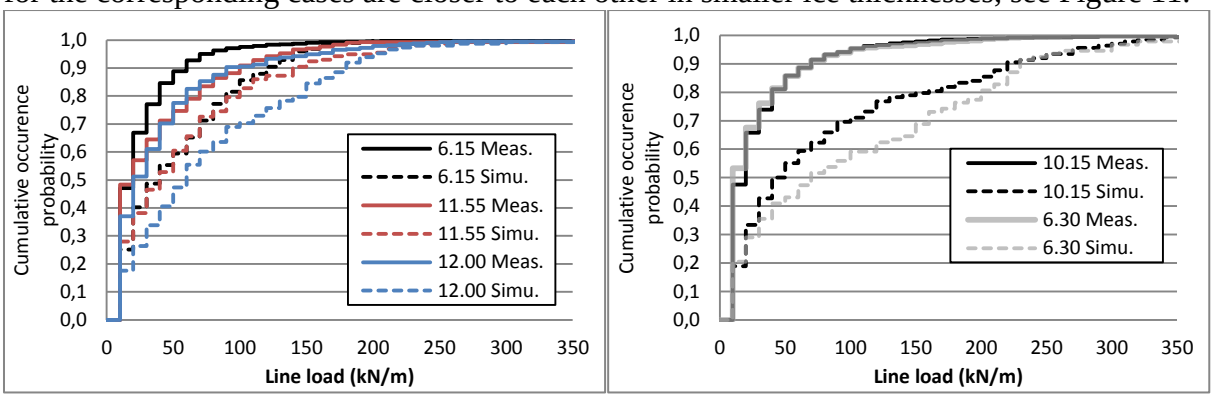

Figure 11. The cumulative occurrence probability of measured 5-minute ice load histograms and the simulated ice loads. Cases 6.15, 11.55 and 12.00 (ice thicknesses 0.23 m, 0.287 m and 0.348 m respectively) on the left and Cases 10.15 and 6.30 (ice thicknesses 0.41 m and 0.468 m respectively) on the right.

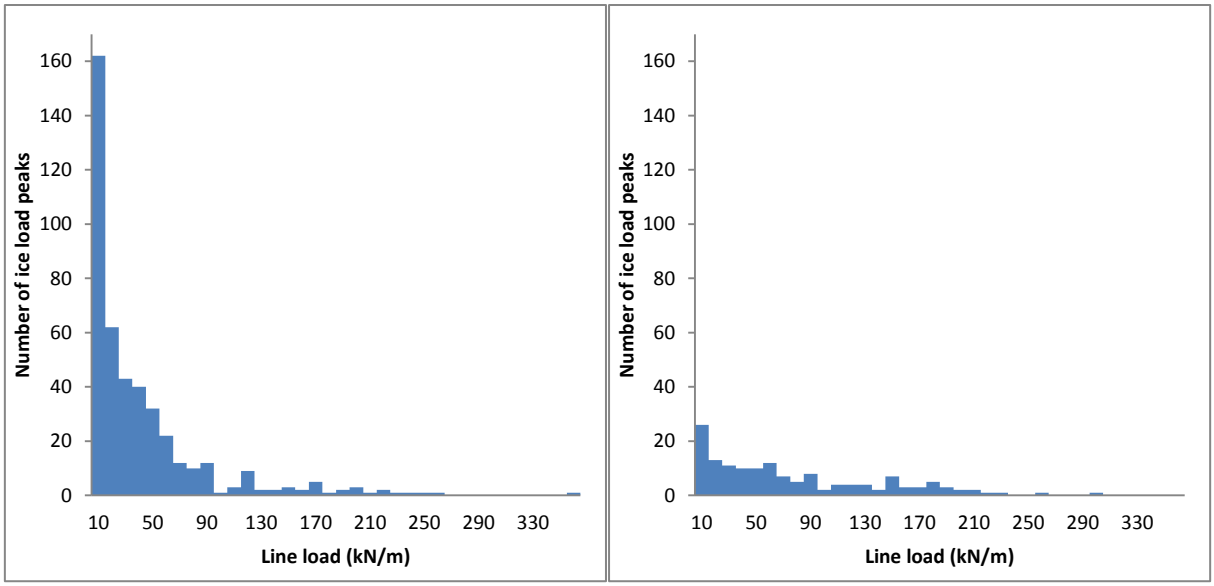

Figure 12 . An example of the measured (on the left) and simulated (on the right) 5-minute ice load histograms (2012-03-21-12.00). The class interval is 10 kN/m and the number indicates the minimum of the class.

As can be seen from Table 5, the simulated mean value, standard deviation and maximum values are increasing with the increasing ice thickness, while the measured ice load values do not follow this trend. This reveals the complexity of actual ice conditions. It can be expected that other ice formations (e.g. ridges), than the level ice simulated here, might be encountered by the vessel during full-scale ice trials. Therefore, a good definition of the corresponding variations of actual ice conditions is crucial for a quantitative comparison between the measured and simulated local ice loads. The comparison shown above must be treated indicative and illustrative as several issues must be verified.

Table 5. Comparison of the measured and simulated 5-minute ice load histograms at bow.

		Measured	Simulated
Case 6.15	Number of peaks	1414	389
	Max (kN/m)	497.40	205.42
	Mean (kN/m)	31.12	57.56
	Standard deviation (kN/m)	31.06	44.40
Case 11.55	Number of peaks	295	156
	Max (kN/m)	356.73	266.14
	Mean (kN/m)	42.24	62.66
	Standard deviation (kN/m)	44.72	55.90
Case 12.00	Number of peaks	436	147
	Max (kN/m)	364.25	304.05
	Mean (kN/m)	46.21	82.15
	Standard deviation (kN/m)	48.47	64.59
Case 10.15	Number of peaks	1117	137
	Max (kN/m)	526.16	347.84
	Mean (kN/m)	35.49	87.01
	Standard deviation (kN/m)	41.10	85.11
Case 6.30	Number of peaks	489	92
	Max (kN/m)	261.98	372.97
	Mean (kN/m)	34.06	107.44
	Standard deviation (kN/m)	38.98	91.50

DISCUSSION

The present numerical model was developed for level ice simulation. The simulated local ice load is the contact (crushing) force between a local hull area and the level ice sheet before it is broken by bending. The local forces induced by the broken ice floes and ambient water are not included in the simulated local ice load histories. Therefore the simulation significantly underestimates the number of smaller ice load peaks as compared with field measurements.

The study showed that the simulation gives plausible results for smaller ice thicknesses. The difference between the measured and simulated values is increasing in greater ice thicknesses as the mean value and standard deviation of the simulated ice loads are significantly higher than the measured ones. The difference might result from the following limitations:

1. The equation of ship motion was not solved in this study, but the measured ship movements were used, which results in a forced course of the ship. As the ship's course is determined, there is no relation between the instantaneous ship's motions and the current ice conditions.
2. The heave, roll and pitch motions were not considered in this simulation.
3. The pressure-area relationship was not considered in this simulation, the current prediction may overestimate local ice loads.
4. The simulated frame loads are the total ice crushing force within a frame area (from top to bottom within the frame spacing), while the measured frame loads might be restricted by sensor locations.

As a summary it can be concluded that the simulation gave plausible results. In the future, the simulation results could possibly be improved, by using the 6DOF simulation program newly developed at CeSOS to solve the ship motions. In addition, taking into account the pressure area relation, the local ice load could be smaller in the simulations and therefore closer to the measured once.

ACKNOWLEDGEMENTS

The authors would like to thank Tekes for the funding of the project. Furthermore, all the project partners, University of Oulu, University of Stellenbosch, Aker Arctic, Rolls-Royce, STX Finland, Wärtsilä, DNV, and the Department of Environmental Affairs of South Africa, are gratefully acknowledged.

REFERENCES

Lindqvist, G., 1989. A straightforward method for calculation of ice resistance of ships. Proceedings of 10th International Conference on Port and Ocean Engineering under Arctic Conditions (POAC 1989), Lulea, Sweden.

Makkonen, L., 2008. Problems in the extreme value analysis. Structural Safety 2008; 30: 405-419.

Su, B., 2011. Numerical predictions of global and local ice loads on ships. Ph.D. thesis, Norwegian University of Science and Technology, Trondheim, Norway.

Su, B., Riska, K., Moan, T., 2010. A numerical method for the prediction of ship performance in level ice. Cold Regions Science and Technology 2010; 60: 177–88.

Su, B., Riska, K., Moan, T., 2011a. Numerical simulation of local ice loads in uniform and randomly varying ice conditions. Cold Regions Science and Technology 2011;65:145–59.

Su, B., Riska, K., Moan, T., 2011b. Numerical study of ice-induced loads on ship hulls. Marine Structures (2011), doi:10.1016/j.marstruc.2011.02.008.